Robotica (2004) volume 22, pp. 205–212. © 2004 Cambridge University Press
DOI: 10.1017/S026357470300554X Printed in the United Kingdom

A simple technique for the autocalibration of stereo systems using the fundamental matrix

Cristian Acevedo and Andrés Guesalaga*

Department of Electrical Engineering, Catholic University of Chile, Santiago, Casilla 306-22 (Chile).
E-mail: aguesala@ing.puc.cl

(Received in Final Form: July 28, 2003)

SUMMARY
This paper presents a method of autocalibrating a stereo system using the full parameterization of the fundamental matrix. The technique is an improvement of classical autocalibration methods that use corresponding points and it is aimed to reduce the number of processes required to achieve a satisfactory calibration. An analysis of the matching points used in the calibration process is carried out in order to select them based upon their quality or reliability. Using this technique, a significant reduction of the convergence errors in the calibration process is obtained.

1. INTRODUCTION

In the last decade, stereoscopy has achieved some interesting results in robotics, autonomous navigation, topographic reconstruction, industrial automation, quality control and medical applications.[1–3]

One of the main disadvantages of this technique is its high sensitivity of 3D reconstruction algorithms to errors in the knowledge of the parameters that model the system and, especially those describing the relative position of the cameras when obtaining the views. This is known as deficient calibration.[4]

The process of calibration consists in the estimation of the parameters that describe the stereoscopic system, and it aims to improve the confidence of 3D measurements.

Earlier works describe various camera calibration methods which differ principally in the information they require for work. These developments can be grouped into two families: Those based on the use of known patterns[5], and the other is autocalibration which requires only feature correspondences between the images.[6,7]

Autocalibration has the advantage of being more autonomous and practical, having also some variants that differ in the way they obtain system parameters[8–12] and the objectives sought in the calibration process.[13,14] An interesting and distinct approach to this method can be found in the literature[7,15] where Kruppa equations[16] are used. However, this is a rather complex approach from a mathematical point of view.

Based on the facts explained above, a new technique that allows for an estimation of the system parameters in a direct manner is introduced. It uses the complete parameterization of the fundamental matrix and relies on a unique method of parameter search.

Autocalibration depends heavily on the estimation precision of the point correspondences in the stereo pair. Problems such as zone occlusions, errors due to texture ambiguity or digitalization, directly influence the precision of the calibration, so a practical implementation is proposed here, using quality factors that ultimately will improve estimation accuracy for autocalibration techniques based on point correspondences.

2. THE MODEL

The model used is the classic pinhole model shown in Figure 1. Point M, located in the 3D space, is projected by a straight line on a retinal plane passing through the optical center at distance f from this plane.

Using the properties of projective geometry,[16] a general relationship can be found between the 3D point M and its projection m on the retinal plane, namely

$$\begin{bmatrix} u*s \\ v*s \\ s \end{bmatrix} = A * \begin{bmatrix} 1 & 0 & 0 & 0 \\ 0 & 1 & 0 & 0 \\ 0 & 0 & 1 & 0 \end{bmatrix} * D * \begin{bmatrix} x \\ y \\ z \\ 1 \end{bmatrix} = P * \begin{bmatrix} x \\ y \\ z \\ 1 \end{bmatrix} \quad (1)$$

with

$$A = \begin{bmatrix} -fk_u & 0 & u_0 \\ 0 & -fk_v & v_0 \\ 0 & 0 & 1 \end{bmatrix} \quad \text{and} \quad D = \begin{bmatrix} R & t \\ 0_3^T & 1 \end{bmatrix}$$

where $[u, v]$ are the projection coordinates of m on the retinal plane, P is the projection matrix, A is the matrix of intrinsic parameters and D is the coordinate transformation matrix from the global origin O to C. It performs a rotation (matrix R) and a translation (vector t), which are also known as extrinsic parameters.

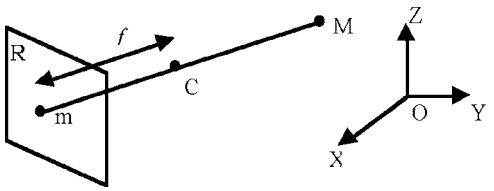


Fig. 1. Pinhole model.

* Corresponding author.

https://doi.org/10.1017/S026357470300554X Published online by Cambridge University Press

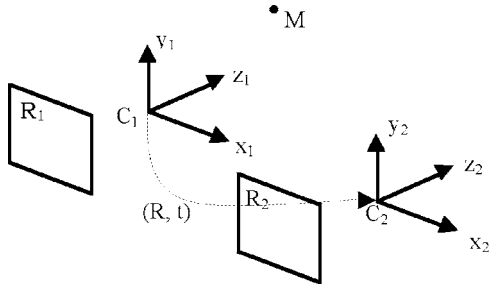


Fig. 2. Displacement between two views.

Defining:

Intrinsic parameters: The first two parameters (*fku*, *fkv*) measure the focal length in terms of pixels and the other two define the projection of the focal center on the retinal plane (*u*0, *v*0).

Extrinsic parameters: Translation vector (*t*1, *t*2, *t*3) and the rotation matrix elements (*yaw y*, *pitch p*, *roll r*) for the three corresponding axis.

2.1. Two views

When a new view is introduced for the same point *M*, there will be two projection equations with independent parameters (if different cameras are used). For simplicity, it is assumed that both views are taken by the same camera (identical intrinsic parameters).

The coordinate system will also be simplified, taking the optical center C_1 of the first view (Figure 2) as the system origin and using the displacement between C_1 and C_2 as the extrinsic parameters.

2.2. Epipolar restriction

Epipolar restriction is one of the most important and powerful results of the stereo vision geometry. A comprehensive analysis can be found elsewhere.[6]

In Figure 3 the basic structure of the epipolar geometry is shown. Points m_1 and m_2 are projections of the 3D point *M* on the retinal planes R_1 and R_2 respectively with C_1 and C_2 being their optical centers which define a straight line whose intersection with the retinal plane form the so called epipoles e_1 and e_2.

Plane Π, defined by *M*, m_1 and m_2, includes all points of the epipolar geometry, and its intersection with the retinal planes R_1 and R_2 define the epipolar lines lm_1 and lm_2, respectively.

Note that only one pair of epipoles, each on a retinal plane, will always exist. When more epipolar lines are drawn, they should intersect with epipoles e_1 and e_2.

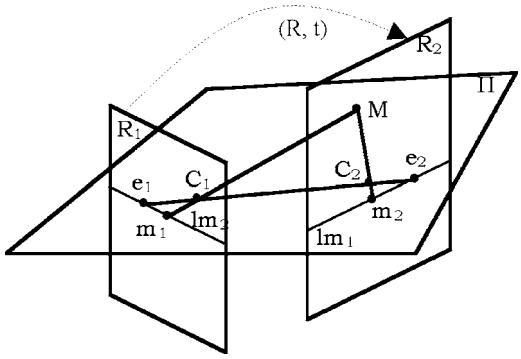


Fig. 3. Epipolar. geometry.

2.3. The fundamental matrix (F)

The epipolar geometry is fully defined by the fundamental matrix, since the latter is formed by functions of all stereo system parameters.

The relationship between the elements of the epipolar geometry and the fundamental matrix generates the following equations.

$$\begin{aligned} lm_1 &= Fm_1 \\ lm_2 &= m_2 F \\ m_2^T * F * m_1 &= 0 \end{aligned} \tag{2}$$

The main importance of the fundamental matrix in the autocalibration process, is that it allows for the estimation of the epipolar geometry and hence, the system parameters.

3. A CRITERION FOR THE ESTIMATION OF F

According to Mohr and Triggs[17], one of the best techniques to estimate the fundamental matrix is the one based on the distance minimization of corresponding points to epipolar lines.

3.1. Definition of the criterion

The basic minimization expression for the estimation of the fundamental matrix is:

$$\sum_i (m_{i2}^T * F * m_{i1})^2 \tag{3}$$

Which can be re-written as:

$$\sum_i (d(m_{i2}, F * m_{i1}))^2 \tag{4}$$

Where function $d(x, l)$ is defined as the Euclidean distance between point *x* and line *l*. The interpretation of (3) is the summation of the distances between the points and their corresponding epipolar lines to those that ideally should belong.

The distance observed between an epipolar line and the corresponding point in the right image in Figure 4, is different from zero because the fundamental does not fully reflects the epipolar geometry of the system. Given that the

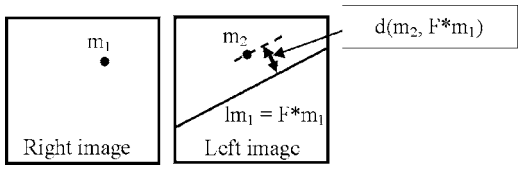


Fig. 4. Distance between corresponding point and epipolar line.

https://doi.org/10.1017/S026357470300554X Published online by Cambridge University Press

described inaccuracy does not exist, point m_2 would be on the epipolar line lm_1. The algorithms based on this idea adjust the fundamental matrix by iteratively reducing the distances between the corresponding points and their epipolar lines, obtaining better estimations of the fundamental matrix. This approximation process is done minimizing expression (3) to an optimum which under ideal conditions should be zero.

However, if the method is applied to the epipolar lines in the second image, the estimation of F could be different for the one obtained for the first image.

Mathematically,

$$\min_F \sum_i (d(m_{i2}, F * m_{i1}))^2 \tag{5}$$

will be different from:

$$\min_F \sum_i (d(m_{i2}^T * F, m_{i1}))^2 \tag{6}$$

This type of incongruity is eliminated incorporating both cases in the minimization problem,

$$\min_F \sum_i (d(m_{i2}, F * m_{i1}) + d(m_{i2}^T * F, m_{i1}))^2 \tag{7}$$

The expression given above can be re-written in its normalized form to avoid scale dependencies[17]:

$$\min_F \sum_i \left(\frac{(m_{i2}^T * F * m_{i1})^2}{(F * m_{i1})_1^2 + (F * m_{i1})_2^2} + \frac{(m_{i2}^T * F * m_{i1})^2}{(m_{i2}^T * F)_1^2 + (m_{i2}^T * F)_2^2} \right) \tag{8}$$

4. PARAMETERIZATION OF THE FUNDAMENTAL MATRIX

When intrinsic and extrinsic parameters are computed from the fundamental matrix, its singularity ($range(F)=2$ defined over a given scale factor) must be considered in order to obtain acceptable values for the binocular system parameters.

There are two alternatives in order to ensure a range 2 for the fundamental matrix:

(i) Minimize over the coefficients of the fundamental matrix under the constraint $range(F)=2$. This option lacks of precision[17].
(ii) Minimizing without constraints on the coefficients of the parameterized fundamental matrix.

4.1. Parameterization as singular matrix

The first and simplest approximation found in literature for a minimization without constraints which considers the main attributes of the fundamental matrix is proposed by Luc Robert[17]:

$$F = \begin{bmatrix} a_1 & a_2 & a_3 \\ a_4 & a_5 & a_6 \\ a_7a_1 + a_8a_4 & a_7a_2 + a_8a_3 & a_7a_3 + a_8a_6 \end{bmatrix} \tag{9}$$

The main characteristic of this approach is that the third row is a linearly dependent of the first two rows, forcing F to be singular ($det(F)=0$).

Next, a simple counter-example is presented for a fundamental matrix representing perfectly parallel pair of cameras, i.e.

$$F_{parallel} = \begin{bmatrix} 0 & 0 & 0 \\ 0 & 0 & k \\ 0 & -k & 0 \end{bmatrix} \tag{10}$$

with k an arbitrary scale factor.

Last row in $F_{parallel}$ cannot be a linear function of the first two, and no combinations of coefficients $a_1, \ldots, a_8$ can adjust to $F_{parallel}$ with the proposed parameterization.

4.2. Parameterization with finite epipoles

A better approach to the previous problem is proposed in previous work[17–19]. Here, the essential features of the fundamental matrix are captured by:

$$F = \begin{bmatrix} b & a & -ay_1 - bx_1 \\ -d & -c & cy_1 + dx_1 \\ dy_2 - bx_2 & cy_2 - ax_2 & -cy_1y_2 - dy_2x_1 + ay_1x_2 + bx_1x_2 \end{bmatrix} \tag{11}$$

Where the corresponding coordinates of the epipoles (x_1, y_1) and (x_2, y_2) in images 1 y 2 are used as parameters.

Note that the last row is linearly dependent to the first two rows and the last column is also a linear function of the first two columns.

Like in the previous case, this model does not behave correctly for perfectly parallel cameras, where common epipole coordinates tend to infinity, generating a numerically unstable estimation.

5. FULL PARAMETERIZATION OF THE FUNDAMENTAL MATRIX

The fundamental matrix F can be decomposed in [reference [7]

$$F = (A^{-1})^T * T * R * A^{-1} \tag{12}$$

where F is a 3×3 matrix.

As mentioned above, the parameterization provide the task of integrating the properties of the matrix F into the estimation process.

In this work, a complete parameterization of the fundamental matrix is proposed, which is achieved by doing all

https://doi.org/10.1017/S026357470300554X Published online by Cambridge University Press

matrix multiplications in a symbolic form, using only the system parameters (intrinsic and extrinsic) as inputs.

The *Fundamental Matrix Generation Function* (*FMGF*), $\Phi(\pi)$, is defined as:

$$\Phi(\pi)=\begin{bmatrix} \varphi_{11} & \varphi_{12} & \varphi_{13} \\ \varphi_{21} & \varphi_{22} & \varphi_{23} \\ \varphi_{31} & \varphi_{32} & \varphi_{33} \end{bmatrix} \tag{13}$$

where π is the vector of system parameters: $\pi=(fku, fkv, u_0, v_0, t1, t2, t3, y, p, r)$.

Every coefficient φ_{ij} in *FMGF* will be non-linear and dependent on the values of the other coefficients. Obviously, any expressions using *FMGF* components will inherit its non-linearity.

6. DIRECT ESTIMATION OF THE INTRINSIC AND EXTRINSIC PARAMETERS

Although classical parameterizations of the fundamental matrix allow for its estimation via a minimization without constraints, they require the computation of their intrinsic parameters using Kruppa equations and subsequently the extrinsic parameters via factorization of matrix *F*.[7]

This disadvantage has led us to develop a new technique to estimate the intrinsic and extrinsic parameters, also via an unconstraint minimization but taking advantage of the recently defined *FMGF*. By doing so, every fundamental matrix will comply with restrictions imposed by the epipolar geometry and their intrinsic and extrinsic parameters will be known *a priori*, eliminating the need to estimate them.

The autocalibration processes described in the literature are based strictly in the estimation of the fundamental matrix starting from point matches. Our proposal can be summarized as an autocalibration based on the direct estimation of the intrinsic and extrinsic parameters starting from point correspondences directly.

The process called *direct estimation of the intrinsic and extrinsic parameters* is shown in Figure 5. Here, the computation of a given criterion allows to estimate the fundamental matrix for the complete set of corresponding points. This criterion is based on the *distance between points and their epipolar lines* which despite being highly nonlinear can be used successfully in conjunction with the *FMGF*. The main idea behind this, is to use the system parameters as the numeric dominion in the minimization of the criterion mentioned above.

7. IMPROVING THE SEARCH FOR POINT CORRESPONDENCES

The autocalibration and 3D reconstruction largely depend on the quality of the matching points, i.e. the accuracy of the point coordinates. To achieve good correspondences, several techniques can be found in the literature, but they can be coarsely divided into two categories:

(i) Improvement in accuracy by subpixel interpolation.

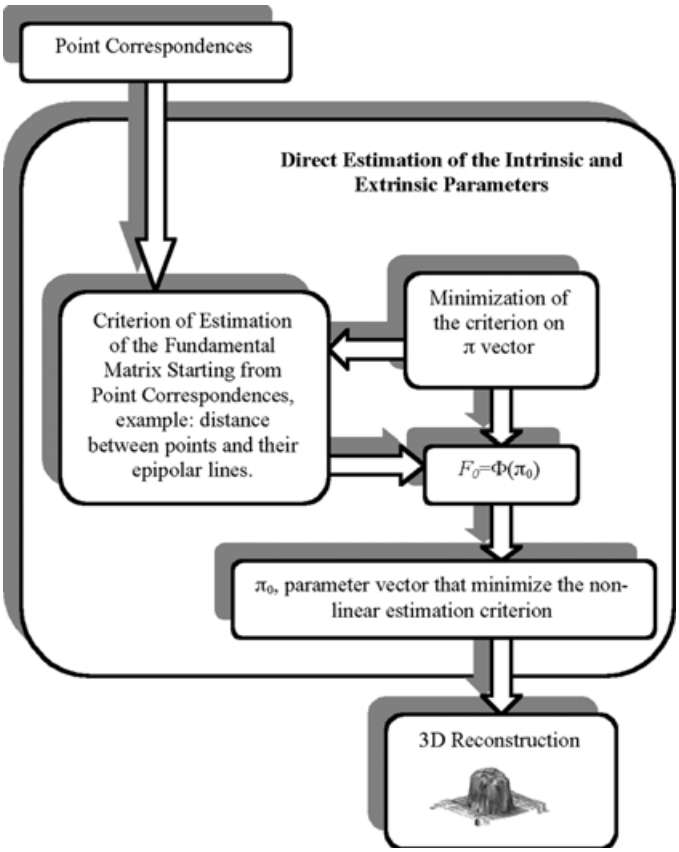


Fig. 5. Direct estimation of intrinsic and extrinsic parameters.

(ii) Improvement in the confidence of correspondences via a characterization of the searching process.

The first group brings together the techniques that allows for a better identification of the corresponding point. An example can be a corner sought in a flat object. In this case, the technique looks for vertices by edge interpolation, achieving subpixel precision in the estimation of the point of interest.

In the second category, methods of point discrimination are included. Here, calibration algorithms and 3D reconstruction techniques are applied to the points that comply with certain specific features, for example a high correlation value.

7.1. Improvement by point discrimination

The simplest way to discriminate points with unsatisfactory quality is by eliminating those points with lower correlation. This technique can be very useful in images where background brightness is uneven or where occlusion occurs. However, this criterion does not identify points with important ambiguities (repetitive patterns), or images with rather flat textures. These cases can contain points of high correlation, but with low reliability due to neighboring points with similar correlation levels.

Figure 6 shows different search cases generating three correlation maps with particular characteristics.

(i) Low correlation maximum.
(ii) High correlation maximum but ambiguous due to repetitive pattern.
(iii) High quality point.

https://doi.org/10.1017/S026357470300554X Published online by Cambridge University Press

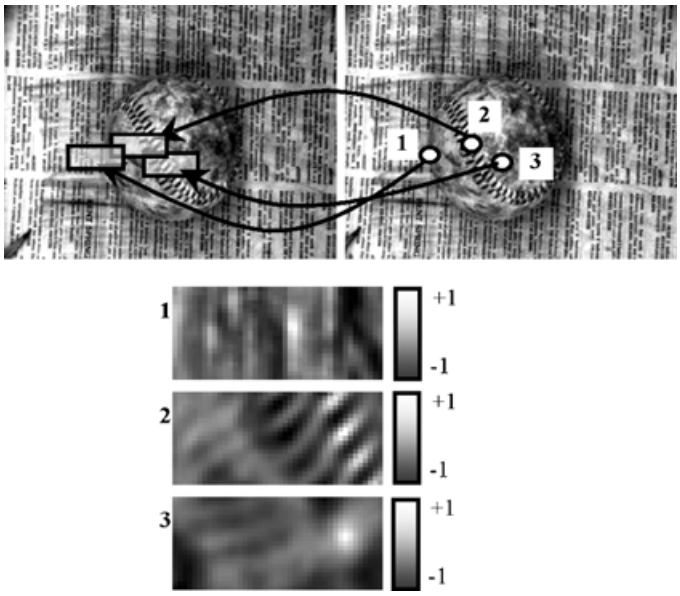


Fig. 6. Examples of the distinct types of correspondences.

Here, the first two cases should be rejected because of their low correlation and ambiguousness.

7.2. Computation of the confidence factor (level of ambiguity)

The computation of the level of ambiguity can be done in a very simple manner using the confidence factor defined in reference [4], expanded for correspondence search in two dimensions.

Based on the original idea, two peaks on the correlation map should be identified, the highest and the second highest. The two values will determine the degree of ambiguity in the search. The more similar the values of the two peaks, the lower the confidence of correspondence.

In those areas where texture is repetitive, for example the seam of the ball in Figure 6 (point 2), a correlation map with various peaks is obtained. Hence, a confidence factor is defined for the first and second maximum in Figure 7:

$$W = 1 - \frac{G_2}{G_1} \tag{14}$$

Notice that the closer the values of the two peaks, the lower the confidence factor.

8. EXPERIMENTAL RESULTS

In this section some results obtained with the previous technique are shown for simulated and real data.

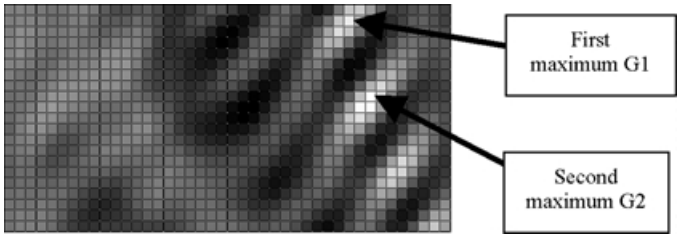


Fig. 7. Map of correlation ambiguity.

The implemented criterion is based on the distances between points and their epipolar lines. As seen earlier, the fundamental matrix has been changed for *FMGF*.

$$\min_{\pi} \sum_{i} \times$$

$$\left(\frac{(m_{i2}^T * \Phi(\pi) * m_{i1})^2}{(\Phi(\pi) * m_{i1})_1^2 + (\Phi(\pi) * m_{i1})_2^2} + \frac{(m_{i2}^T * \Phi(\pi) * m_{i1})^2}{(m_{i2}^T * \Phi(\pi))_1^2 + (m_{i2}^T * \Phi(\pi))_2^2} \right) \tag{15}$$

with $\pi \in \Re^{10} - \{0\}$ and $\Phi(\pi)$ *FMGF*.

The expression shown above (criterion) is the objective function of the minimization and vector π is the operation variable. In the ideal optimum, the objective function should be zero, however, under real conditions its value remains strictly positive and is referred as the estimation error.

8.1. Simulated environment

For algorithm validation via simulation, a system of synthetic projections with uniformly distributed points within a controlled volume is generated for a pair of virtual cameras. The system generates 500 points in two retinal planes with double precision coordinates.

Different camera arrangements were tested and it was found that the most difficult parameters to detect are those closer to the singular case in which both cameras are parallel to each other.

Table I contains the parameters for a different case, i.e. near a parallel configuration. After extensive simulation with different values, this case showed to be one of the harshest to converge (Figure 8).

Tests were carried out using high precision in coordinate values, so quantization problems were negligible. It was found, however, that the algorithm is not immune to the location of cameras. The main results are presented in Table II.

8.2. Real images

In this case, real images are used with *a priori* knowledge of some basic features of the cameras (both views were taken with the same camera). Distance (baseline or t_1) between views is also known.

Among the extrinsic parameters, the most difficult to estimate is the angle of convergence (yaw). It is desirable then, to work on images where this value is important.

Table I. Parameters for simulated case.

Feature	Value
Baseline	20
($t1$, $t2$, $t3$)	(20, 0.1, 0.1) mm
(*yaw*, *pitch*, *roll*)	(0.2, 0.1, 0.1) degrees
Image size	256 x 237 pixels
(*fku*, *fkv*)	(1470, 1460)
($u0$, $v0$)	(127.5, 118)

https://doi.org/10.1017/S026357470300554X Published online by Cambridge University Press

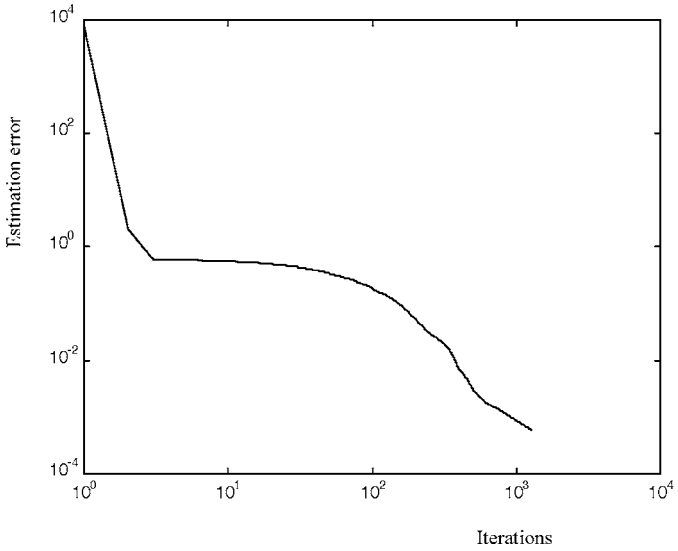


Fig. 8. Error convergence (simulation).

Table II. Results of the autocalibration process (simulated case).

Feature	Value
Number of points	500
Initial error	7816.82
Final error	0.00061
Iterations	433

Parameters

Intrinsic	Initials	Finals	Actual
fku [*pixels*]	1454.54	1466.32	1470
fkv [*pixels*]	1454.54	1457.41	1460
*u*0 [*pixels*]	127.5	128.12	127.5
*v*0 [*pixels*]	118	117.32	118

Extrinsic

*t*1 [*mm*]	20	20	20
*t*2 [*mm*]	0	0.099	0.1
*t*3 [*mm*]	0	0.101	0.1
yaw [°]	0	0.189	0.2
pitch [°]	0	0.107	0.1
roll [°]	0	0.0998	0.1

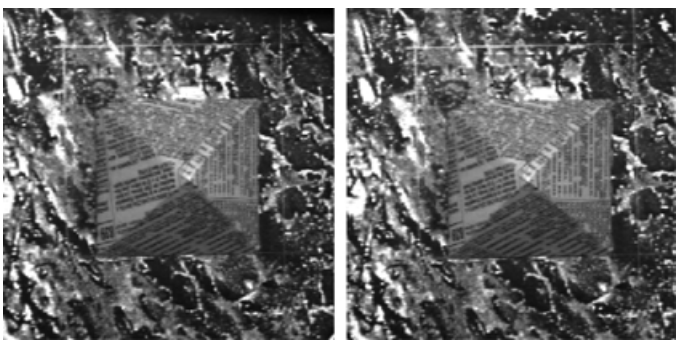


Fig. 9. Views of a pyramid with yaw=5°.

The object used for experimentation was a pyramid wrapped in newspaper, lying over a flat surface rich in texture (Figure 9). The main parameters used for the this setting are defined in Table III.

A total of 500 points, uniformly distributed on the image were computed for the convergence process. As Figure 10 shows, the method converges rapidly (Table IV).

The results of the autocalibration process turned out to be very close to the arbitrary values set previously (Table V). The most important value (*yaw*), originally measured at 5°, was estimated in 5.3°. In spite of being a very stiff estimation problem, the result is acceptable thanks to the implicit subpixel precision used.

8.3 The effect of quality of corresponding points on the convergence process

In this section, the effect of the quality of corresponding points on calibration convergence is tackled.

Table III. Parameters of the optical setting (real images).

Feature	Value
Baseline	60 mm
(*yaw*, *pitch*, *roll*)	(5 ± 1, 0, 0) degrees
Pixel size	0.011×0.011 mm
Focal length *f*	16 mm
Image size	256×256 pixels
(*fku*, *fkv*)	(1454.54, 1454.54) pixels
(*u*0, *v*0)	unknown

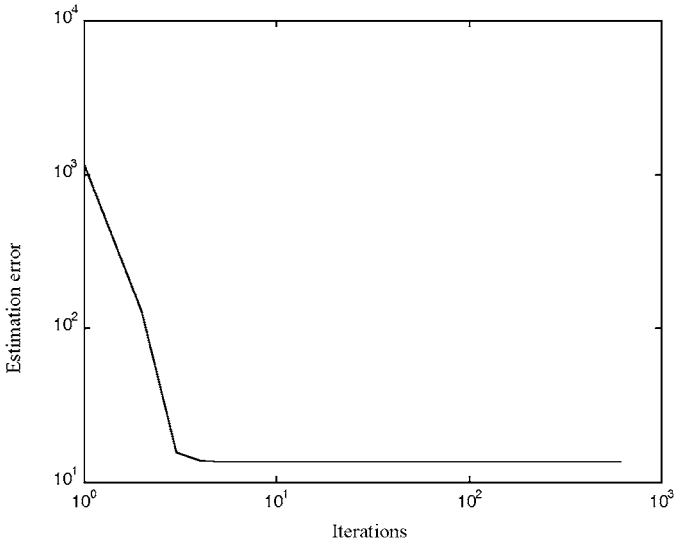


Fig. 10. Error convergence using 500 points (real images).

Table IV. Convergence results (real images).

Feature	Value
Number of points	500
Mean correlation	0.916
Mean confidence	0.994
Initial error	1136.79
Final error	13.55
Iterations	608

https://doi.org/10.1017/S026357470300554X Published online by Cambridge University Press

Table V. Initial and final parameters (real images).

Parameters			
Intrinsic	Initials	Finals	Actual
fku [*pixeles*]	2181.81	1530.50	1454.54
fkv [*pixeles*]	2181.81	1602.31	1454.54
*u*0 [*pixeles*]	127.5	125.47	unknown
*v*0 [*pixeles*]	127.5	127.5	unknown
Extrinsic			
*t*1 [*mm*]	60	60	60
*t*2 [*mm*]	0	0.00495	0
*t*3 [*mm*]	0	0.1689	0
yaw [°]	0	5.297	5
pitch [°]	0	–0.0268	0
roll [°]	0	–0.0028	0

The stereo pair shown in Figure 6 has been used. Here, occlusion zones and areas with periodic texture could clearly introduce errors in the estimation of the correspondences.

Four sets of samples for the correspondence search were selected, each with very distinctive characteristics. The points selected in each case are shown in Figure 11.

Set 1 was taken randomly, without any analysis of the selected points. Set 2 was also taken in a randomly manner, but those points below the limits of 0.7 for maximum correlation and 0.2 for confidence factor were eliminated. These points were replaced until completing a full set of 500 points.

Set 3 contains points with factors over thresholds 0.9 and 0.65 in order to improve the quality of the correspondence points substantially. Notice that the points selected are concentrated over a reduced sector. This could eventually limit the information they provide for calibration purposes.

Looking for a balance between the quality of points and their spatial distribution, a selection procedure for correspondence points based on equal zones was developed (Set 4). The reference image (right image) was divided into 100 identical areas and a search was done for the best points in each one of them, achieving a uniform density and similar quality indexes.

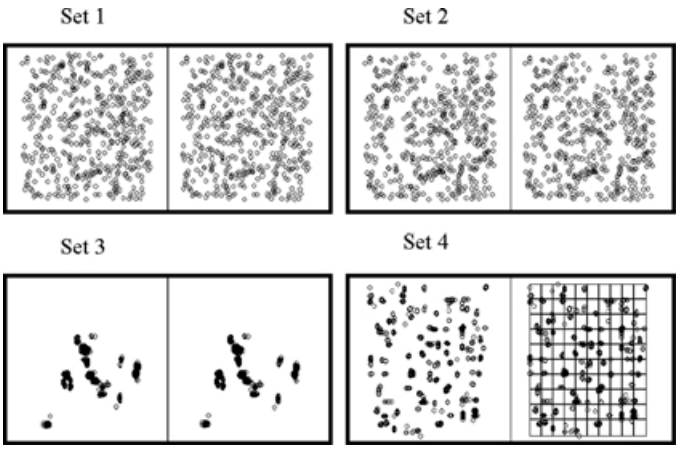


Fig. 11. Selected points for convergence.

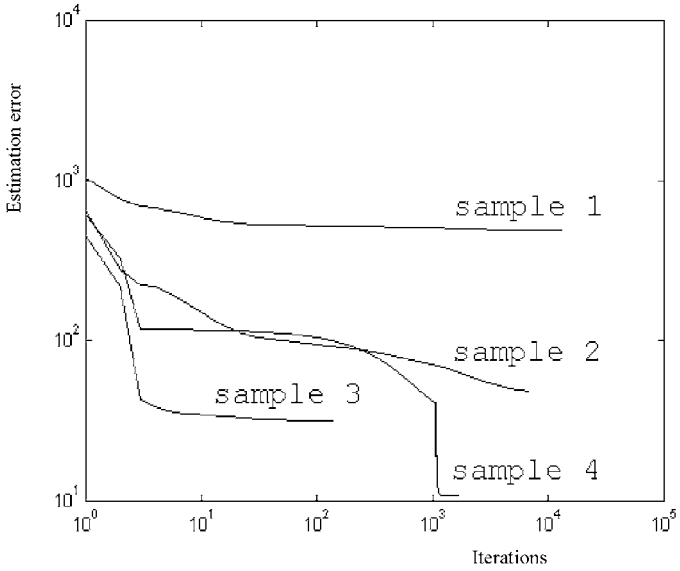


Fig. 12. Error convergence using 500 points (four sets).

Table VI. Convergence results for different correspondence qualities.

Feature	Set 1	Set 2	Set 3	Set 4
Number of points	500	500	405	500
Mean correlation	0.866	0.896	0.935	0.931
Mean confidence	0.329	0.379	0.687	0.457
Initial error	1044.48	643.33	559.10*	608.21
Final error	485.93	48.28	39.52*	10.89
Iterations	13386	6807	140	1725

The convergence process is plotted in Figure 12 where set 4 clearly attains a superior performance.

Notice that only 405 points for sample 3 were found for the specified thresholds. The values in stars were scaled by a factor of 500:405 so that they were comparable with other values in Table VI.

9. CONCLUSIONS

In this paper an autocalibration process based in the complete parameterization of the fundamental matrix has been shown. However, this development involves various contributions:

- Development of a new estimation criterion of the intrinsic and extrinsic parameters based on the complete parameterization of the fundamental matrix.
- Significant reduction of computations involved in estimating system parameters, i.e. Kruppa equations and factorization of the fundamental matrix have been eliminated.
- Improvement in the accuracy of the autocalibration process based on the new criterion that incorporates the confidence factor.
- A method of selecting the best corresponding points for calibration, which is based on quality estimators and spatial distribution of these points.

The first two contributions considerably reduce the complexity involved in the estimation of the intrinsic and extrinsic parameters.

https://doi.org/10.1017/S026357470300554X Published online by Cambridge University Press

The last two contributions reduce the autocalibration errors significantly. Given that the method is based on corresponding points, the characterization and improvement in their quality allows a faster and better convergence. For the example shown in Figure 12 a reduction of 97.7% in the final error is attained using a technique that activates only high quality points in the specified zones.

The intrinsic limitation in the autocalibration process is mainly due to the fact that the fundamental matrix is defined on a scale factor. This means that autocalibration will estimate the translation vector as a directional vector without magnitude, introducing an error in the 3D reconstruction. This error is proportional to the scale factor, and the limitation created can be overcome by using a "yard stick" or a benchmark contained in the images. This reference will allow for a correction in the real scale of the object.

Acknowledgements
The authors thank Fondecyt (project 1990105) for sponsoring this work.

References

1. J. Weber, D. Koller, Q. Luong and J Malik, "An Integrated Stereo-Based Approach to Automatic Vehicle Guidance," *Proceedings of the Fifth International Conference on Computer Vision*, Cambridge, MA (1995) pp. 52–57.
2. O. Faugeras, S. Laveau, L. Robert, G. Csurka and C. Zeller "3-D Reconstruction of Urban Scenes from Sequences of Images," *Rapport de Recherche* No. 2572, INRIA, Sophia Antipolis, France (June, 1995).
3. J. P. Duclos and Andrés Guesalaga, "Recovery of the Optic Disc Structure Using Stereoscopic Techniques," *International Conference on Signal Processing Application & Technology*, San Diego, CA (1997) pp. 363–367.
4. M. A. Torres and Andrés Guesalaga, "Confidence Factor and Adaptive Disparity Range for Reliable 3D Reconstruction," *Computational Intelligence for Modelling & Automation Control*, Vienna, Austria (1999) pp. 83–90.
5. R. Tsai, "A Versatile Camera Calibration Technique for High Accuracy 3D Machine Vision Metrology Using Off-the-Shelf TV Cameras and Lenses," *IEEE Journal of Robotics and Automation* **3**(4), 323–344 (August, 1987).
6. O. Faugeras, *Three-Dimensional Computer Vision: A Geometric Viewpoint* (The MIT Press. Cambridge, Massachusetts, USA, 1993).
7. Q. Luong and O. Faugeras, "Self-Calibration of a Stereo Rig from Unknown Camera Motion and Point Correspondences," *Rapport de Recherche* No. 2014, INRIA, Sophia Antipolis, France (July, 1993).
8. R. Horaud, G. Csurka and D. Demirdjian, "Stereo Calibration from Rigid Motions," *Rapport de Recherche* No. 3496, INRIA, Sophia Antipolis, France (January, 1998).
9. J. Lawn and R. Cipolla, "Reliable Extraction of the Camera Motion using Constraints on the Epipole," *Proceedings of the Fourth European Conference on Computer Vision*, Cambridge, UK (1996) pp. 161–173.
10. L. Robert, "Camera Calibration without Feature Extraction," *Rapport de Recherche* No. 2204, INRIA, Sophia Antipolis, France (February, 1994).
11. T. Viéville and D Lingrand, "Using Singular Displacement for Uncalibrated Monocular Visual System," *Rapport de Recherche* No. 2678, INRIA, Sophia Antipolis, France (1995).
12. Z. Zhang, Q. Luong and O Faugeras, "Motion of an Uncalibrated Stereo Rig: Self-Calibration and Metric Reconstruction," *Rapport de Recherche* No. 2079, INRIA, Sophia Antipolis, France (October, 1993).
13. Z. Zhang, R. Weiss and A. Hanson, "Automatic Calibration and Visual Servoing for a Robot Navigation System," *Proceedings of the IEEE International Conference on Robotics and Automation* Atlanta, Georgia (1993) pp. 14–19.
14. Z. Zhang, R. Deriche, O.Faugeras and Q. Luong, "A Robust Technique for Matching Two Uncalibrated Images Trough the Recovery of the Unknown Epipolar Geometry," *Rapport de Recherche* No. 2273, INRIA, Sophia Antipolis, France (May, 1994).
15. C. Zeller and O. Faugeras, "Camera Self-Calibration from Video Sequences: the Kruppa Equations Revisited," *Rapport de Recherche* No. 2793, INRIA, Sophia Antipolis, France (February, 1996).
16. R. Mohr and B. Triggs, "Projective Geometry for Image Analysis," *Tutorial given at International Symposium of Photogrammetry and Remote Sensing*, Vienna (July, 1996).
17. Q. Luong, R. Deriche, O. Faugeras and T. Papadopoulo, "On Determining the Fundamental Matrix: Analisis of Different Methods and Experimental Results," *Rapport de Recherche* No. 1894, INRIA Sophia Antipolis, France (April, 1993).
18. G. Csurka, C. Zeller, Z. Zhang and O. Faugeras, "Characterizing the Uncertainty of the Fundamental Matrix," *Rapport de Recherche* No. 2560, INRIA Sophia Antipolis, France (June, 1995).
19. Z. Zhang, "Determining the Epipolar Geometry and it Uncertainty: A Review," *Rapport de Recherche* No. 2927, INRIA Sophia Antipolis, France (July, 1996).

https://doi.org/10.1017/S026357470300554X Published online by Cambridge University Press